Ligand Identification in Titanium Complexes Using X-ray Valence-to-Core Emission Spectroscopy

ARTICLE *in* INORGANIC CHEMISTRY · SEPTEMBER 2010

Impact Factor: 4.76 · DOI: 10.1021/ic100755t · Source: PubMed

6 AUTHORS, INCLUDING:

Kalaivani Seenivasan
Stella Maris College
12 PUBLICATIONS **132** CITATIONS
SEE PROFILE

Carlo Lamberti
Università degli Studi di Torino
379 PUBLICATIONS **13,009** CITATIONS
SEE PROFILE

Pieter Glatzel
European Synchrotron Radiation Facility
202 PUBLICATIONS **5,059** CITATIONS
SEE PROFILE

Inorganic Chemistry
Article

Inorg. Chem. 2010, 49, 8323–8332 8323
DOI: 10.1021/ic100755t

Ligand Identification in Titanium Complexes Using X-ray Valence-to-Core Emission Spectroscopy

Janine C. Swarbrick,*,† Yaroslav Kvashnin,† Karina Schulte,‡ Kalaivani Seenivasan,§ Carlo Lamberti,§ and Pieter Glatzel†

†*European Synchrotron Radiation Facility (ESRF), BP 220, F-38043, Grenoble, Cedex 9, France,* ‡*MAX-Lab, Lund Universitet, Ole Römersväg 1, 223 63 Lund, Sweden, and* §*Department of Inorganic, Physical and Materials Chemistry and NIS Centre of Excellence and INSTM Reference Center, University of Turin, Via P. Giuria 7, I-10135 Turin, Italy*

Received April 20, 2010

The identification of ligands in metalloorganic complexes is crucial for understanding many important biological and chemical systems. Nonresonant Kβ valence-to-core X-ray emission spectroscopy (XES) has been demonstrated as a ligand identification technique which is complementary to other spectroscopies, such as X-ray absorption. In this study we show the Kβ valence-to-core XES alongside the Ti K-edge X-ray absorption near edge structure spectra for a series of chemically relevant low-symmetry Ti organometallic complexes. The spectra are modeled using density functional theory calculations. XES spectra are analyzed in terms of the molecular orbitals probed, in order to understand the effects of bond length, bond nature, orbital hybridization, and molecular symmetry on the observed spectral features.

Introduction

Ligand identification plays a key role in understanding a wide range of systems, from protein binding sites[1,2] and drug activity[3] to catalytic processes.[4] The recently reported technique of using chemically sensitive nonresonant Kβ valence-to-core X-ray emission spectroscopy (XES) has successfully been used to determine the ligands in solid-state Cr[5,6] and molecular Mn systems.[7,8] The technique has several advantages. It is element specific so the spectra can be recorded for the atom (and ligands) of interest. It is also hard X-ray based, thus there are few limitations on the sample environment, making high-pressure studies or studies of liquid systems easily feasible. Such a ligand-sensitive technique, without strict restrictions on the sample environment, can find application in several important studies which require in situ changes to be followed, such as monitoring ligand binding in catalytic reactions or tracking ligand conformation changes occurring during biological processes. Monitoring transformations in such systems is possible under real conditions using this powerful technique.

XES measurements can be achieved using a synchrotron radiation source and an X-ray emission spectrometer and involves a core 1s electron being excited into the continuum. The core hole is filled by an electron relaxation which results in a fluorescence photon being emitted. The Kβ valence-to-core lines (Figure 1), from predominantly metal 4p and ligand np to metal 1s (K$\beta_{2,5}$ peak) and ligand ns to metal 1s (Kβ'' peaks) transitions, relate to the ligands and the chemical environment of the atom being studied.[8] It is the Kβ'' peak which has been used as a ligand identification peak. The separation of the Kβ'' from the K$\beta_{2,5}$ peak at higher energy was shown to follow the same trend as the ligand ns binding energy, and the Kβ'' peak intensity was found to increase with decreasing metal−ligand bond distance.[8]

Recently Smolentsev et al.[7] published a comprehensive account of the valence-to-core XES spectra of a series of model Mn compounds, where they demonstrate that spectral

*To whom correspondence should addressed. E-mail: janine.grattage@esrf.fr. Telephone: +33(0)4 38 88 19 30.

(1) Glaser, F.; Morris, R. J.; Najmanovich, R. J.; Laskowski, R. A.; Thornton, J. M. *Proteins: Struct., Funct., Bioinf.* **2006**, *64*, 479–488.
(2) Perera, R.; Sono, M.; Sigman, J. A.; Pfister, T. D.; Lu, Y.; Dawson, J. H. *Proc. Natl. Acad. Sci. U.S.A.* **2003**, *100*, 3641–3646.
(3) Klekota, B.; Miller, B. L. *Trends Biotechnol.* **1999**, *17*, 205–209.
(4) Bordiga, S.; Damin, A.; Bonino, F.; Zecchina, A.; Spano, G.; Rivetti, F.; Bolis, V.; Prestipino, C.; Lamberti, C. *J. Phys. Chem. B* **2002**, *106*, 9892–9905.
(5) Safonov, V. A.; Vykhodtseva, L. N.; Polukarov, Y. M.; Safonova, O. V.; Smolentsev, G.; Sikora, M.; Eeckhout, S. G.; Glatzel, P. *J. Phys. Chem. B* **2006**, *110*, 23192–23196.
(6) Eeckhout, S. G.; Safonova, O. V.; Smolentsev, G.; Biasioli, M.; Safonov, V. A.; Vykhodtseva, L. N.; Sikora, M.; Glatzel, P. *J. Anal. At. Spectrom.* **2009**, *24*, 215–223.
(7) Smolentsev, G.; Soldatov, A. V.; Messinger, J.; Merz, K.; Weyhermüller, T.; Bergmann, U.; Pushkar, Y.; Yano, J.; Yachandra, V. K.; Glatzel, P. *J. Am. Chem. Soc.* **2009**, *131*, 13161–13167.
(8) Bergmann, U.; Horne, C. R.; Collins, T. J.; Workman, J. M.; Cramer, S. P. *Chem. Phys. Lett.* **1999**, *302*, 119–124.

Published on Web 08/17/2010

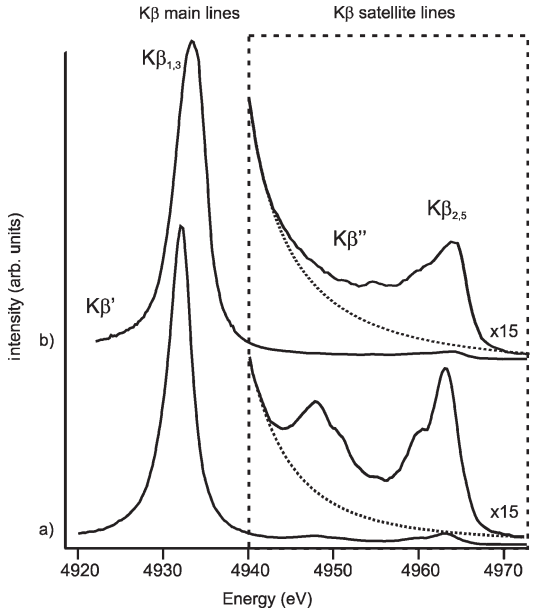

Figure 1. Kβ emission lines for (a) TiOPc ($S = 0$) and (b) $Ti(THF)_3Cl_3$ ($S = 1/2$) showing the separate spectral components. Both compounds are low spin and so no Kβ' peak is seen. The Kβ main line of $Ti(THF)_3Cl_3$ is broader and at a higher energy than that of TiOPc, consistent with $Ti(THF)_3Cl_3$ having a higher spin state.[9] The background (later subtracted) is indicated with a dashed line on the right of the figure for the two spectra.

intensity can be calculated by integrating the core- and valence-state matrix elements using the relation:

$$I(E_i) \simeq \sum_{j=1}^{3} |\langle \Psi_{1s} | \mathbf{e}_j \mathbf{r} | \Psi_{MOi} \rangle|^2 \qquad (1)$$

where Ψ_{1s} and Ψ_{MOi} are the wave functions of the core 1s state and i^{th} valence molecular orbital (MO) state with energy E_i, $\mathbf{e}_j$ is an orthogonal set of unit vectors, and $\mathbf{r}$ is a position vector. Since the 1s state has A_1 symmetry, spectral intensity is seen only if the MO also has symmetry which gives a nonzero transition product (dependent on the point group symmetry). This relation can be used to see, based on understanding the symmetry present, whether or not Kβ'' peaks will appear in the valence-to-core XES spectrum or whether the peak will be suppressed as being symmetry forbidden.

In this study a series of Ti organometallic compounds with C, N, O, and Cl ligands was investigated to understand how the bond type and the nature of the ligand atom in Ti metalloorganic complexes affects the valence-to-core XES and Ti K-edge X-ray absorption near edge structure spectra (XANES). The samples studied have low point group symmetry and none have inversion symmetry: TiOPc has the highest order symmetry, (C_{4v}), then Cp_2TiCl_2 and $Ti(THF)_2Cl_4$ (C_{2v}), then $TiPcCl_2$ (close to C_{2v}) and the others have C_1 symmetry. Based on eq 1, some spectral intensity is expected from all atoms of those with C_1 symmetry. For a molecule with C_{4v} symmetry, orbitals with A_1 or E (but not A_2, B_1, or B_2) symmetry will give spectral intensity, and for molecules with C_{2v} symmetry, orbitals with A_1, B_1, and B_2 (but not A_2) symmetry will give spectral intensity. To understand the origin of the observed peaks, including their shape, intensity, and energy position, density functional theory (DFT) calculations performed using the ORCA code[12] have been used to model the measured spectra. Each calculated spectral component relates to a different MO which can also be generated from the calculated Kohn−Sham orbitals and provides a useful visualization of the location of electron density over the molecule at each calculated energy.

Alongside the valence-to-core XES measurements, the Ti K-edge XANES spectra were also recorded for all samples, which probes the unoccupied states just above the Fermi level and can be used to understand the local coordination of the Ti atom. The post edge features are due to 1s−4p and 1s−continuum transitions. The pre-edge arises from 1s−3d quadrupolar transitions only in systems with strict inversion symmetry. If this symmetry is not present, as for the molecules studied here, then p−d orbital mixing can occur, and the pre-edge features can become dominated by 1s−4p dipolar transitions which are around 100 times stronger than quadrupolar transitions.

Where the pre-edge in K-edge XANES provides information on the unoccupied valence states, the valence-to-core XES probes the occupied valence states and also accesses the ligand effects of the central metal atom. As demonstrated in this manuscript, the valence-to-core XES spectra can also be readily calculated using DFT using a relatively simple model (neglecting the core-hole effects).

Titanium complexes are of interest in several research fields, and determining how the various ligands interact with the central Ti atom is crucial to understand how these molecules behave in the reactions and the processes taking place. Titanyl phthalocyanine (TiOPc) and titanium phthalocyanine dichloride ($TiPcCl_2$) are studied for application in organic light-emitting diodes (OLEDs) and photovoltaic devices.[13−15] $TiPcCl_2$ is often used as a reaction precursor for titanium organometallic molecular synthesis, such as dyads[16] and other axially substituted systems.[17] Cyclopentadienyl titanium trichloride (Cp-$TiCl_3$), the methylated form, pentamethylcyclopentadienyl titanium trichloride (PMCp−$TiCl_3$), and dichlorobis (indenyl) titanium (BisIn-$TiCl_2$) are used as homogeneous polymerization catalysts.[18−21] Dichlorobis (cyclopentadienyl) titanium (titanocene dichloride, Cp_2TiCl_2) is of interest in cancer treatment and reached stage II clinical trials.[22] Derivatives are now being investigated as improved antitumor agents.[23] $Ti(THF)_2Cl_4$ and $Ti(THF)_3Cl_3$

(9) Glatzel, P.; Bergmann, U. *Coord. Chem. Rev.* **2005**, *249*, 65–95.
(10) Hayashi, H.; Takeda, R.; Udagawa, Y.; Nakamura, T.; Miyagawa, H.; Shoji, H.; Nanao, S.; Kawamura, N. *Phys. Scr.* **2005**, *T115*, 1094–1096.
(11) Hämäläinen, K.; Siddons, D. P.; Hastings, J. B.; Berman, L. E. *Phys. Rev. Lett.* **2005**, *67*, 2850–2853.
(12) Neese, F. *ORCA, an ab initio DFT and semiempirical electronic structure package*, version 2.7, University of Bonn: Bonn, Germany, 2009.
(13) Hohnholz, D.; Steinbrecher, S.; Hanack, M. *J. Mol. Struct.* **2000**, *521*, 231–237.
(14) Adams, D. M.; Kerimo, J.; Olson, E. J. C.; Zaban, A.; Gregg, B. A.; Barbara, P. F. *J. Am. Chem. Soc.* **1997**, *119*, 10608–10619.
(15) Tsuzuki, T.; Kuwabara, Y.; Noma, W.; Shirota, Y.; Willis, M. R. *Jpn. J. Appl. Phys., Part 2* **1996**, *35*, L447–L450.
(16) Ballesteros, B.; de la Torre, G.; Torres, T.; Hug, G. L.; Rahman, G. M. A.; Guldi, D. M. *Tetrahedron* **2006**, *62*, 2097–2101.
(17) Barthel, M.; Dini, D.; Vagin, S.; Hanack, M. *Eur. J. Org. Chem.* **2002**, *22*, 3756–3762.
(18) Alt, H. G.; Koppl, A. *Chem. Rev.* **2000**, *100*, 1205–1221.
(19) Tsai, J. C.; Kuo, J. C.; Chen, Y. C. *J. Polym. Sci., Part A-1: Polym. Chem.* **2005**, *43*, 2304–2315.
(20) Jany, G.; Gustafsson, M.; Repo, T.; Aitola, E.; Dobado, J. A.; Klinga, M.; Leskela, M. *J. Organomet. Chem.* **1998**, *553*, 173–178.
(21) Gibson, V. C.; Spitzmesser, S. K. *Chem. Rev.* **2003**, *103*, 283–315.
(22) Köpf-Maier, P. *Eur. J. Clin. Pharmacol.* **1994**, *47*, 1–16.

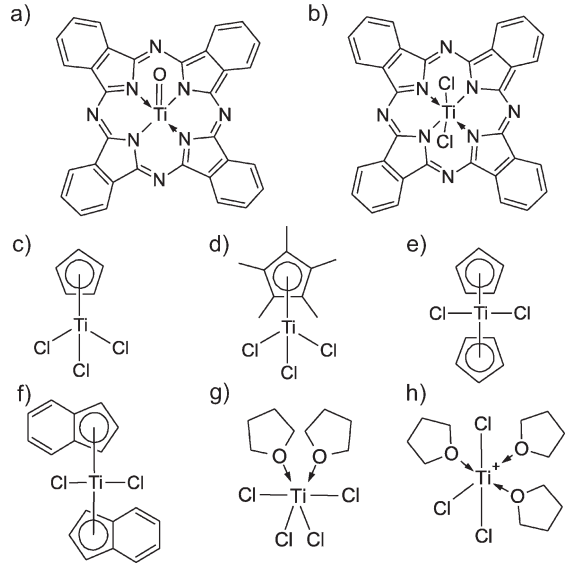

Figure 2. Molecules studied: (a) TiOPc, (b) $TiPcCl_2$, (c) $Cp-TiCl_3$, (d) $PMCp-TiCl_3$, e) Cp_2TiCl_2, f) $BisIn-TiCl_2$, g) $Ti(THF)_2Cl_4$, and h) $Ti(THF)_3Cl_3$.

(THF = tetrahydrofuran) are used as precursors for a new generation of Ziegler−Natta polymerization catalysts.[24]

The molecules studied are shown in Figure 2. $TiPcCl_2$ and TiOPc are both off-planar phthalocyanine (Pc) molecules with axial ligands. TiOPc has an apical O atom double bonded to the Ti, perpendicular to the molecular plane. $TiPcCl_2$ has two Cl atoms bonded to Ti in a cis geometry. Cp-$TiCl_3$ and PMCp-$TiCl_3$ both have a Ti atom bonded to three Cl atoms on one side, with a Cp or PMCp ring bonded opposite the Cl atoms, giving a "piano stool" configuration. Cp_2TiCl_2 has two Cp rings and two Cl atoms bonded to the central Ti atom. BisIn-$TiCl_2$ is similar to Cp_2TiCl_2, but each ring is replaced by an indenyl moiety. $Ti(THF)_2Cl_4$ and $Ti(THF)_3Cl_3$ are six-fold-coordinated molecules with Cl ligands and THF ring groups bonded to the Ti through the O atoms.

Methods

The experiments were performed on the high brilliance X-ray emission beamline ID26 at the ESRF. The electron energy was 6.0 GeV with a ring current of 170−200 mA. The incident energy was selected by means of a pair of cryogenically cooled Si(311) single crystals. Higher harmonics were suppressed using two Si mirrors at 2.5 mrad. The beam size was approximately 1 mm horizontally and 0.3 mm vertically. The analyzer used for Ti Kβ emission detection exploits the (331) Bragg reflection of a spherically bent, 1 m bending radius Ge crystal in the vertical Rowland geometry with a Bragg angle of ~75°, giving an overall resolution taken from the full width at half-maximum (fwhm) of the elastic peak of 0.9 eV. The emitted photons were measured using a 100 μm avalanche photodiode (APD). Ti K-edge high energy resolution fluorescence detected (HERFD) XANES spectra were measured by monitoring the absorption over the Ti K-edge using the Ti $K\beta_{1,3}$ emission line intensity to reduce spectral broadening arising from the core hole lifetime.[9−11] Use of an APD detector gives zero background counts in the XANES spectra. Between approximately 300−1000 counts per second are detected at the peak of the Ti $K\beta_{2,5}$ line for these concentrated samples.

All samples except $Ti(THF)_2Cl_4$ and $Ti(THF)_3Cl_3$ were prepared by grinding dry crystals into a powder with boronitride (for binding) in a 4:1 ratio before pressing the homogeneous mixture into a 5 mm diameter pellet for mounting in a liquid He cooled cryostat in the beam. To avoid the contamination of the air-sensitive $Ti(THF)_2Cl_4$ and $Ti(THF)_3Cl_3$ samples, these were measured inside sealed capillaries (1.0 mm in diameter), following the well-established procedure adopted for X-ray powder diffraction (XRPD)[25] and extended X-ray absorption fine structure spectroscopy (EXAFS)[26,27] experiments. All compounds were purchased from Sigma Aldrich and used without further purification, except $Ti(THF)_2Cl_4$ and $Ti(THF)_3Cl_3$ which were kindly supplied by Istituto Guido Donegani, Novara (Italy). A single isomer was measured of each of these two molecules. For $Ti(THF)_3Cl_3$ only one isomer is reported to exist.[33] For $Ti(THF)_2Cl_4$, two isomers have been reported, and in this experiment, the more stable cis isomer was isolated and measured,[34] as confirmed using XRPD and UV−visible techniques.

Radiation damage tests were carried out by monitoring the shape and position of the Ti K pre-edge by rapidly recording (10 s scans) XANES spectra using a photodiode (to obtain the maximum detector efficiency). The time taken until a change was seen between two consecutive spectra was taken as the time until the sample suffered radiation damage. Therefore all spectra were recorded for a time less than this radiation damage time limit, after which a fresh sample spot was used.

The XES experimental spectra have had the background subtracted by fitting the Kβ main peak at 4933 eV with four Voigt peaks. Four Voigt peaks were chosen as being enough to give a close fit to the Kβ main line and the Kβ valence-to-core spectral background. The tail of this fit is shown as the Kβ valence-to-core spectral background in Figure 1. The spectra are all calibrated to the incident energy scale using the elastic peak measured at the same time as the valence-to-core XES spectra.

For the calculations, the input geometry was taken from published crystallographic data (for TiPcO,[28] $TiPcCl_2$,[29] Cp-$TiCl_3$,[30] PMCp-$TiCl_3$,[31] Cp_2TiCl_2,[32] $Ti(THF)_2Cl_4$,[33] and $Ti(THF)_3Cl_3$).[34] No structural data was available for BisIn-$TiCl_2$, therefore, calculations for this molecule are based on a theoretical model of a single molecule, with a geometry minimized via molecular mechanics then optimized within DFT. To calculate the Kβ valence-to-core spectrum, the ORCA code written by Neese et al. was used.[12] ORCA is a density functional code which can be used to calculate the nonresonant XES spectra by calculating the transitions from occupied states to the 1s core hole. It can also calculate the

(23) Abeysinghe, P. M.; Harding, M. M. *Dalton Trans.* **2007**, *32*, 3474–3482.
(24) Bordiga, S.; Bonino, F.; Damin, A.; Lamberti, C. *Phys. Chem. Chem. Phys.* **2007**, *9*, 4854–4878.
(25) Turnes Palomino, G.; Bordiga, S.; Zecchina, A.; Marra, G. L.; Lamberti, C. *J. Phys. Chem. B* **2000**, *104*, 8641–8651.
(26) Estephane, J.; Groppo, E.; Vitillo, J. G.; Damin, A.; Gianolio, D.; Lamberti, C.; Bordiga, S.; Quadrelli, E. A.; Basset, J. M. *J. Phys. Chem. C* **2010**, *114*, 4451–4458.
(27) Gianolio, D.; Groppo, E.; Vitillo, J. G.; Damin, A.; Bordiga, S.; Zecchina, A.; Lamberti, C. *Chem. Commun.* **2010**, *46*, 976–978.
(28) Okada, O.; Oka, K.; Iijima, M. *Jpn. J. Appl. Phys., Part 1* **1993**, *32*, 3556–356.
(29) Goedken, V. L.; Dessy, G.; Ercolani, C.; Fares, V.; Gastaldi, L. *Inorg. Chem.* **1985**, *24*, 991–995.
(30) Engelhardt, L. M.; Papasergio, R. I.; Raston, C. L.; White, A. H. *Organometallics* **1984**, *3*, 18–20.
(31) Pevec, A. *Acta Chim. Slov.* **2003**, *50*, 199–206.
(32) Nieger, M.; Hupfer, H. *CCDC Database*, private communication, contribution from the Department of Inorganic Chemistry, University of Bonn: Bonn, Germany, 1999; number CCDC 113637.
(33) Lis, T.; Ejfler, J.; Utko, J.; Sobota, P. *Pol. J. Chem.* **1992**, *66*, 93.
(34) Handlovič, M.; Mikloš, D.; Zikmund, M. *Acta Crystallogr., Sect. B: Struct. Sci.* **1981**, *37*, 811–814.

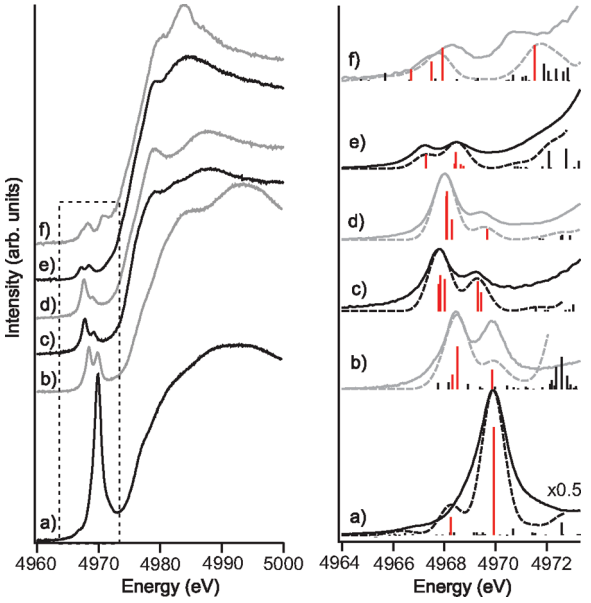

Figure 3. Left: HERFD XANES spectra of (a) TiOPc, (b) $TiPcCl_2$, (c) Cp−$TiCl_3$, (d) PMCp−$TiCl_3$, (e) Cp_2TiCl_2, and (f) BisIn−$TiCl_2$. Right: Pre-edge regions of these spectra (solid line) alongside ORCA calculated pre-edge peaks with 1 eV broadening (dashed line). Spectra were normalized to the edge jump in the EXAFS region.

pre-edge components in XAS spectra by considering transitions from unoccupied levels just above the Fermi level to a 1s core hole. Ground-state DFT calculations have been shown to be a good approximation for valence-to-core XES spectra calculations as the effect of the core hole is screened by the metal 3d valence electrons, which do not strongly affect the spectra.[7] The calculations were performed using a triple-ζ polarized basis set[35] using the Becke−Perdew BP86 as an exchange and correlation functional, with a finer grid and flexible CP(PPP) basis set over the Ti absorber, and as a further geometry refinement; optimization of the hydrogen atoms (while keeping the other atoms frozen) was performed. Tight self-consistent field convergence criteria were applied, and all molecules (except $Ti(THF)_3Cl_3$ which has spin $S = 1/2$ and spin multiplicity, $2S + 1$, of 2) were considered to have spin $S = 0$, multiplicity 1. All calculated models were of neutral charge. For $Ti(THF)_3Cl_3$, spin-state effects were investigated in the calculations and were found to have little influence on the spectra.

Results

Ti K-edge HERFD XANES. The high energy resolution fluorescence detection (HERFD) spectra for all compounds (excluding $Ti(THF)_2Cl_4$ and $Ti(THF)_3Cl_3$) are shown in Figure 3, normalized to the edge jump in the EXAFS region at higher energy. The spectra for $Ti(THF)_2Cl_4$ and $Ti(THF)_3Cl_3$ are not included here, as these compounds suffered radiation damage relatively quickly, and as such, good statistics in the pre-edge region were not obtained. The pre-edge region of the recorded spectra are shown in detail on the right of the figure alongside DFT calculations, both the individual calculated components (sticks) and the spectra after applying 1 eV Gaussian broadening to the calculated components. The principal peak components are highlighted in red and detailed in Table 1 in the Supporting Information). The calculations are in good agreement overall with the measured spectra. Aside from TiOPc which has a single strong pre-edge peak, the other compounds have a split pre-edge of lower overall intensity. The strong pre-edge peak in TiOPc arises from relatively high Ti p−d mixing (12.0% p-type orbital in the main pre-edge peak), which is possible from the square planar (C_{4v}) molecular symmetry. The 1s electron transitions to p orbitals are about 100 times stronger than to d orbitals, therefore, a small increase in the amount of p orbital gives a significant increase in peak intensity in p−d mixed pre-edge peaks. The other compounds calculated also have p−d mixing in the pre-edge, as they also do not exhibit inversion symmetry. However the proportion of p orbitals in these peak components is calculated to be lower (up to a maximum 5.6% for Cp-$TiCl_3$), giving lower overall intensity. The multipeak pre-edges are split because of the low molecular symmetry present, separating the unoccupied MOs in energy. The measured spectra, pre-edge calculations and d orbital assignments are in agreement with those previously reported for Cp-$TiCl_3$ and Cp_2TiCl_2[36] and for PMCp-$TiCl_3$.[37]

As suggested in ref 36, the decrease in p orbital contribution to the weaker pre-edge features does not arise from the molecular symmetry being close to having inversion symmetry (thus forbidding p−d mixing), because all the compounds have low symmetries and no inversion centers. The effect of the ligands on the Ti atoms is understood to cause the reduction in Ti p-type orbitals in the pre-edge. Thus using valence-to-core XES spectroscopy, which is sensitive to the ligand atoms, can be used to better understand the ligand effects on the central Ti species.

Kβ XES Measurements. The Kβ valence-to-core XES for the Ti complexes are shown in Figure 4. The $K\beta_{2,5}$ peak for TiOPc is seen at 4963.2 eV and for $TiPcCl_2$ is slightly higher at 4963.4 eV. The $K\beta_{2,5}$ main peaks for Cp-$TiCl_3$ and PMCp-$TiCl_3$ are at 4963.0 eV and for Cp_2TiCl_2 and BisIn-$TiCl_2$ at 4962.5 eV. The $K\beta_{2,5}$ peak of $Ti(THF)_2Cl_4$ is at 4964.9 eV and that of $Ti(THF)_3Cl_3$ at 4964 eV. The TiOPc $K\beta_{2,5}$ peak has a clear shoulder at 4960 eV and a significant Kβ'' feature with peaks at 4948 and 4950.7 eV. For all four Cp ring and Cl-containing samples, there are Kβ''-range features around 4953 eV and at lower energy at 4948 eV. $TiPcCl_2$ shows the fewest features with no distinct peaks in the Kβ'' region. $Ti(THF)_2Cl_4$ and $Ti(THF)_3Cl_3$ have Kβ'' peaks at 4955 eV and some intensity lower in energy at 4947 eV.

Since all the compounds have relatively low symmetry, extensive orbital mixing takes place which in turn splits the orbital contributions to the spectral peaks, giving broader features overall. Unlike previous studies using the Kβ'' peak as a ligand identifier,[5,7] for these Ti complexes it appears that directly bonded ligand atoms do not necessarily give rise to clear Kβ'' peaks.[38] No clearly

(35) Schafer, A.; Horn, H.; Ahlrichs, R. *J. Chem. Phys.* **1992**, *97*, 2571–2577.

(36) DeBeer George, S.; Brant, P.; Solomon, E. I. *J. Am. Chem. Soc.* **2004**, *127*, 667–674.

(37) Wasserman, E. P.; Westwood, A. D.; Yu, Z.; Oskam, J. H.; Duenas, S. L. *J. Mol. Catal. A: Chem.* **2001**, *172*, 67–80.

(38) Pushkar, Y.; Long, X.; Glatzel, P.; Brudvig, G. W.; Dismukes, G. C.; Collins, T. J.; Yachandra, V. K.; Yano, J.; Bergmann, U. *Angew. Chem., Int. Ed.* **2010**, *49*, 800–803.

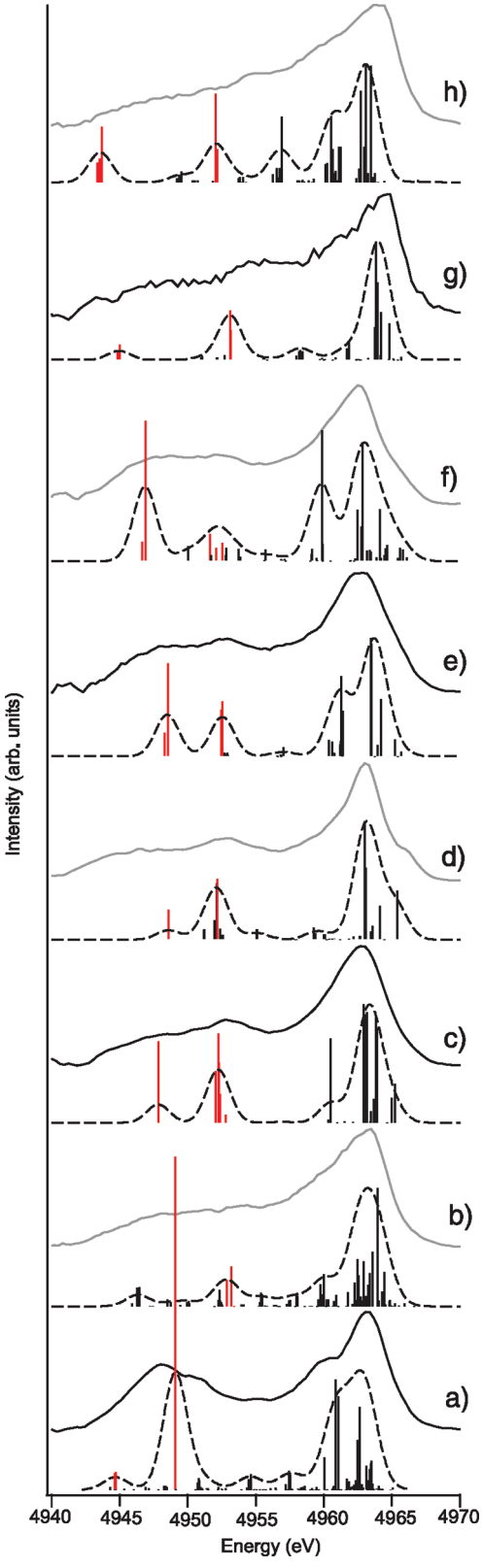

Figure 4. Experimental spectra compared to the DFT calculated Kβ valence-to-core spectra (2.0 eV broadening) with components shown: (a) TiOPc, (b) $TiPcCl_2$, (c) $Cp-TiCl_3$, (d) $PMCp-TiCl_3$, (e) Cp_2TiCl_2, (f) $BisIn-TiCl_2$, (g) $Ti(THF)_2Cl_4$, and (h) $Ti(THF)_3Cl_3$. Calculations of compound (f) are based on a theoretically determined molecular geometry. Spectra are normalized to the intensity of the K$\beta_{2,5}$ peak. The MOs corresponding to peak contributions in red have significant Ti p and ligand s components and are shown later.

identifiable Kβ'' peaks are seen in the experimental trace for $TiPcCl_2$, yet the Ti atom has N and Cl atoms bonded directly to it, which show low-intensity peaks in the calculated spectrum. There is also only one clear Kβ'' peak in the four Cp ring/indenyl molecules ($Cp-TiCl_3$, $PMCp-TiCl_3$, Cp_2TiCl_2, and $BisIn-TiCl_2$), with some broad spectral intensity lower in energy. These four compounds have both C and Cl ligands, therefore, we may expect two peaks from the C and Cl atoms. For the two THF and Cl containing molecules ($Ti(THF)_2Cl_4$ and $Ti(THF)_3Cl_3$), one Kβ'' peak is seen in the experimental data at a similar energy to a peak in the Cp ring/indenyl molecules, thus we may initially suggest this peak arises from Cl ligands. No clear Kβ'' peak is seen due to the O atoms in the THF rings, although there is a strong Kβ'' peak seen for TiOPc which is found to be due to the O atom. The DFT calculated spectra can be used to determine the origin of the spectral features and understand the criteria for the presence of Kβ'' peaks in these Ti molecular systems.

Kβ Valence-to-Core XES Calculations. The background-subtracted measured and calculated spectra are shown in Figure 4, with applied broadening parameters of 2.0 eV to simulate the broadening of the measured spectra due to the experimental energy bandwidth and other small effects not included in the theoretical model. The individual calculated spectral contributions are also shown. It should be noted that it is a common problem in the calculations of valence-to-core spectra using DFT that the theoretically calculated transitions have to be broadened by an amount that exceeds the values of experimental and core-hole lifetime broadening. There is to date no strict theoretical analysis of the underlying mechanisms. The simplified theoretical approach presented in this manuscript neglects the core-hole effect, multi-electron excitations, and only considers a finite number of atoms. A detailed study of these effects on the valence-to-core spectra is beyond the scope of the present manuscript.

Overall the calculations give a good fit to the experimental data. The inclusion of quadrupolar transitions has no visible effect on the calculated spectra, thus the spectra reflect the p − density of states (DOS), as found previously.[7] By comparing the calculated and measured spectra, the origin (atom and orbital type) of the different peaks can be assigned. Peaks appear in the Kβ'' region of the calculated spectra where the contributing MOs have both Ti p and ligand s character. The most intense contributions to the Kβ'' peaks are shown in Figure 4 in red. Each of these is discussed alongside the MO it corresponds to. These MOs are calculated in terms of the proportion of each atomic orbital (AO) for the constituent atoms, thus the importance of orbital hybridization can be determined in relation to the presence of Kβ'' features. For each MO shown for a molecule with higher than C_1 symmetry, the symmetry subgroup of the MO is given in the tables included in the Supporting Information.

Phthalocyanine Molecules. The Kβ valence-to-core spectrum of TiOPc has the most prominent Kβ'' peaks. The calculations show that the smaller contribution at (a calculated value of) 4944.5 eV originates from two degenerate MOs with N 2s, C 2s, and Ti $3p_{x/y}$ character.

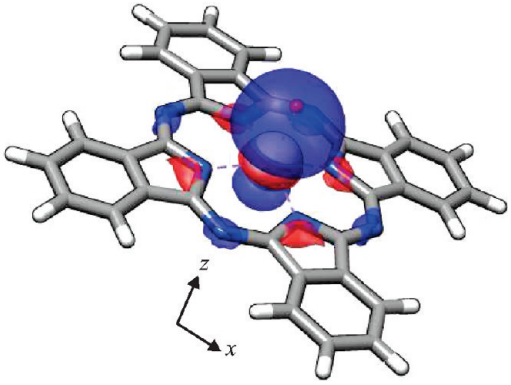

Figure 5. MO of TiOPc contributing to the strong Kβ'' peak. It is assigned to O and Ti only and is thus highly localized.

The strong peak at 4949.1 eV is from a MO with mainly (77.9%) O 2s with Ti p_z character. This orbital has a relatively high orbital hybridization between O 2s and Ti $3p_z$ (plus Ti 3s and $3d_z^2$ AO), and little delocalization over other neighboring atoms, which is why the spectral feature is so strong. The MO is shown in Figure 5 with peak components shown in the Supporting Information, Table 2.

The strong O 2s related Kβ'' peak arises from electrons relaxing back to the Ti 1s orbital from a very pure Ti−O MO shown in Figure 5, which is in part due to the symmetry of the molecule. The apical oxygen atom lies along the z axis along with the Ti p_z orbital, giving strong hybridization between the Ti p_z and O s orbitals. Additionally the double bond between the Ti and O gives a relatively short Ti−O distance of 1.64 Å,[39] which acts to increase the intensity of the O Kβ'' peak according to eq 1. Conversely, due to the constraints of the *Pc* framework, the Ti−N distance is 2.08 ± 0.02 Å,[39] which is relatively long compared with other Ti−N containing compounds,[40] acting to reduce the hybridization between N 2s and Ti 3p orbitals and to weaken the Kβ'' peak intensity due to N. The orbitals with N 2s character hybridize, though not strongly, with Ti 3p, C and N $2p_x$ and $2p_y$ orbitals over an energy range of a few eV. This gives several weak contributions with some N character, thus no clear peak is seen due to N atoms.

Symmetry arguments are also useful to understand the presence of O and N Kβ'' peaks in the case of TiOPc (which has C_{4v} symmetry). From eq 1 and symmetry arguments (for a comprehensive summary of molecular symmetries also see http://www.staff.ncl.ac.uk/j.p.goss/symmetry/index.html), it can be seen that there will only be spectral intensity if the core 1s state (with A_1 symmetry), and the MO from which an electron relaxes to fill the core hole also has some proportion of A_1 or E symmetry. In the case of TiOPc, the O based MO shown in Figure 5 has A_1 symmetry and thus results in spectral intensity. Such arguments can be similarly followed for the other molecules, where the symmetry of the relevant orbitals is noted in the tables and shows that transitions from these orbitals are symmetry allowed. No symmetry implies C_1 molecular point group symmetry, i.e., all transitions are allowed.

(39) Zakharov, A. V.; Shlykov, S. A.; Zhabanov, Y. A.; Girichev, G. V. *Phys. Chem. Chem. Phys.* **2009**, *11*, 3472–3477.
(40) Gross, M. E.; Siegrist, T. *Inorg. Chem.* **1992**, *31*, 4898–4899.

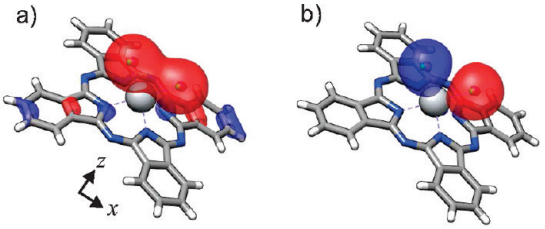

Figure 6. MOs of $TiPcCl_2$ contributing to the very weak Kβ'' feature due to Cl s orbitals.

Possible limitations of the DFT calculation method are seen in the case of TiOPc, where the calculated and experimentally observed peaks are not in as strong agreement as for the other compounds. The calculations are performed on the molecule in the ground state, therefore, any core-hole relaxation effects are omitted. No multielectron effects are accounted for in the calculations which may cause differences with the measured data. These factors would be present in the spectra of all systems but perhaps only show an effect in the spectra of TiOPc. As a further investigation, calculations were performed for TiOPc in different crystal structures and for molecular clusters of different sizes (from one to four molecules), and little difference is seen for these variations. Details of the additional calculations are included in the Supporting Information. It can be concluded from these cluster calculations that valence-to-core XES spectra are dominated by local effects chiefly relating to the metal atom being probed and to the directly bonded ligands. The extended crystal structure appears to have little influence on the measured spectra.

For the $TiPcCl_2$ molecule, first it is interesting to note that the structure determined experimentally[29] is different to that calculated using molecular mechanics methods for a single molecule. Crystallographic data shows the *Pc* plane to be twisted by a small amount, with the two axial Cl atoms pointing toward the neighboring molecule. In the theoretically optimized structure of a single molecule, the Cl atoms are located such that the Cl−Ti−Cl plane is perpendicular to the *Pc* plane. Using the two different geometries in the DFT input, different XES spectra are calculated as the MOs change. The experimentally determined structure is used here as it gives a better comparison with the measured spectrum and is a more realistic representation of the measured sample.

In contrast to TiOPc, the measured $TiPcCl_2$ spectrum shows no individual clear Kβ'' peaks, which may be expected due to the axial Cl atoms, since the strong peak in TiOPc is due to the apical O atom. On inspection of the DFT calculations, the two MOs with the strongest Cl 3s character are shown in Figure 6. Peak components are shown in Table 3 in the Supporting Information. The MOs with N 2s character in the $TiPcCl_2$ calculations also have significant hybridization with C, H, and Cl orbitals. Orbitals with strong Cl 3s character are shown in Figure 6 but only give a low-intensity peak in the calculations, which is due to the molecular geometry. Unlike TiOPc, the axial Cl atoms in $TiPcCl_2$ do not share an axis of symmetry with a Ti p-type orbital, and since the orbitals which have Cl s character do not also have both Ti $p_{x/y}$ and Ti p_z character, the overall hybridization is relatively weak. For both (Pcs), even the MOs

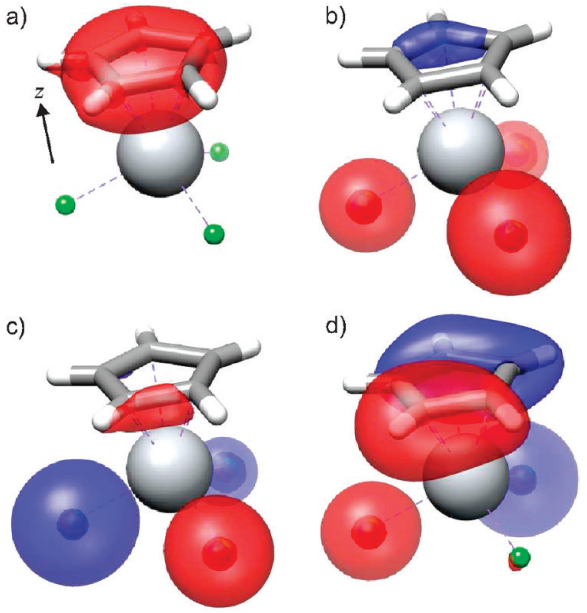

Figure 7. MOs of Cp−$TiCl_3$ giving the main contributions to the Kβ'' peaks from (a) C s orbitals and (b−d) from Cl s orbitals.

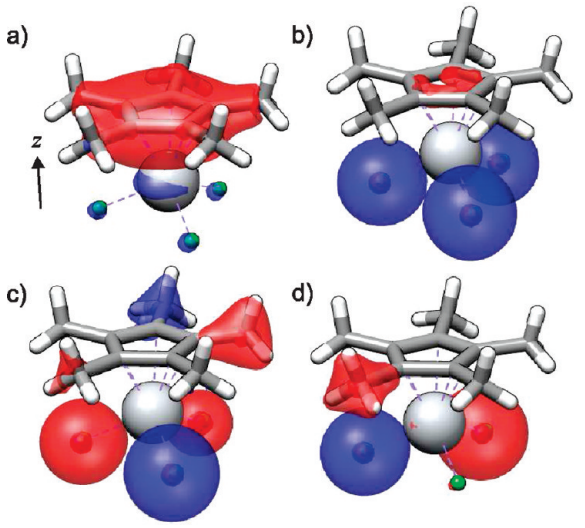

Figure 8. MOs of PMCp−$TiCl_3$ in the Kβ'' peak region from (a) C 2s orbitals and (b−d) Cl 3s orbitals.

with the highest proportion of N 2s orbitals have contributions from all N and C atoms in the molecule and exist over an energy range of a few eV. This delocalization over the C and N atoms in the macrocycle is typical of (Pc) molecules. Therefore, instead of distinct ligand peaks in the Kβ'' range due to N or C, a broad intensity is seen from the relatively large number of hybridized N and C orbitals.

Inspecting the calculated peak contributions for the two *Pc* compounds shows the effect of extensive hybridization on the presence or absence of Kβ'' ligand peaks; both have a similar calculated Kβ'' contribution except for the large single MO in TiOPc from the O 2s /Ti 3p orbital. We conclude that the presence of extensive delocalization in a molecule prevents the clear observation of Kβ'' peaks due to macrocycle atoms, thus revealing a limitation of this spectroscopic technique in ligand identification of highly hybridized systems.

Cp-Ring-Based Ti Molecules. For Cp-$TiCl_3$ the calculated peak at 4947.8 eV is due to an orbital with Ti $3p_z$ (plus Ti 4s and $3d_z^2$ character) and strong C 2s character, i.e., from the Cp ring, see Figure 7a. In the measured data this contribution from C appears as a broad intensity rather than a clear peak. This is explained in terms of the nature of the bond between Ti and the Cp ring (vide infra).

The clearer peak at higher energy (4952.2 eV) is from three MOs, with Ti $3p_{x/y/z}$ character (and Ti 4s character) and strong Cl 3s character over the three Cl atoms, Figure 7b−d. These orbitals give the main contributions to the Kβ'' region (Figure 7) and are from relatively pure MOs which do not spread over several different atoms, only Ti and Cl. There is also significant overlap between the Cl 3s- and Ti 3p-type orbitals due to the low molecular symmetry and the presence of Ti $3p_x$, $3p_y$, and $3p_z$ contributions allowing mixing with the Cl 3s orbitals. The orbital assignment is more straightforward for smaller molecules like Cp-$TiCl_3$, as there are fewer contributing atoms.

The PMCp-$TiCl_3$ calculation shows a similar trend as that seen for Cp-$TiCl_3$ for the Kβ'' peaks. The shoulder to the K$\beta_{2,5}$ at 4966 eV is reproduced in the calculations. The lowest Kβ'' peak at 4946.5 eV arises from an orbital with Ti $3p_z$ as well as Ti 4s and $3d_z^2$ character, with strong C 2s character in a similar way as for Cp-$TiCl_3$ (see Figure 8a). The contribution around 4952 eV is from several MOs, the three strongest of which have some C 2s and strong Cl 3s character with Ti $p_{x/y/z}$ character. These spectral peak assignments are qualitatively and quantitatively similar to those found for Cp-$TiCl_3$ which is expected, as the two molecules are very similar and the only difference involves ligands not directly bound to the Ti atom (methyl groups on the Cp ring).

For these two single Cp-ring molecules we observe the expected Kβ'' peaks due to ligand ns−metal 3p orbital hybridization giving peak intensity. There are features from the C and Cl atoms seen in the measurements and in the calculations. However, the peaks are broader in the measurements, particularly those relating to C atoms, due to hybridization effects which split the energy levels in the real system. As seen for TiOPc, the peaks which are clearest are those from Cl orbitals which have a high proportion of Cl 3s with significant Ti 3p character (a high bond purity), which is evident in the MO plots in Figure 7 and Figure 8.

The calculated peak relating to C 2s for Cp-$TiCl_3$ is of higher intensity than for PMCp-$TiCl_3$. The individual AO contributions from Ti$3p_{x/y/z}$, Cl 3s and C 2s to the low energy C 2s -based MO are almost identical for both molecules (see Supporting Information, Tables 4 and 5), and analysis of the bond lengths show that the Ti−C separation in PMCp-$TiCl_3$ is marginally longer than for Cp-$TiCl_3$ (by 0.06 Å). Neither the proportion of AOs in the C 2s -based MO, nor the difference in Ti−C bond length for each molecule, is enough to account for the relative reduction in intensity of the C 2s Kβ'' peak seen for PMCp-$TiCl_3$ compared with Cp-$TiCl_3$. Upon inspection of the MO diagrams in Figure 7a and Figure 8a, it can be seen that the difference arises due to hybridization of the MO over the ring moiety. In Cp-$TiCl_3$ the MO is

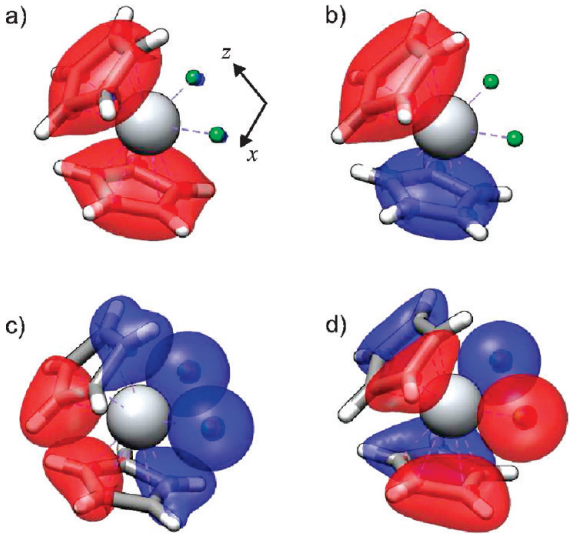

Figure 9. MOs of Cp_2TiCl_2 giving the main contributions to the Kβ'' peaks, from a), b) C s orbitals and c), d) Cl s orbitals.

located over the five C atoms of the Cp ring, whereas for PMCp-$TiCl_3$ the MO is spread over the central Cp ring and also the five outer methyl C atoms. This increased delocalization further away from the central Ti atom in PMCp-$TiCl_3$ acts to reduce the Ti 3p -C2s orbital overlap and thus reduce the intensity of the peak seen in the calculated spectra due to C compared with Cp-$TiCl_3$.

For Cp_2TiCl_2 the broader K$\beta_{2,5}$ peak compared with other molecules is shown in the calculations to arise from a splitting in the contributions to this peak. There are two clear Kβ'' peaks each from two main MO contributions, which reproduce the experimental spectrum very well. The first peak has two contributions with Ti3p_z, and Ti 4s and 3d_{z^2} contributions, with strong C 2s character (Figure 9a) and b)). The stronger overlap between the C 2s and Ti 3$p_{x/y/z}$ orbitals, of twice the number of C atoms in Cp_2TiCl_2 compared with Cp-$TiCl_3$ and PMCp-$TiCl_3$, gives the stronger C Kβ'' peak. The second peak at 4952.6 eV is from two main contributions, both with Ti3$p_{x/y/z}$, strong Cl 3s and C 2s character (Figure 9c) and d)).

The calculations for the valence-to-core XES spectrum BisIn-$TiCl_2$ relate to a theoretical model with a molecular geometry minimized in the DFT calculations, rather than an experimentally determined geometry as with the other molecules. At 4946.7 eV a Kβ'' peak is seen with two spectral components based on C 2s AO contributions hybridized with Ti 3p AO (Figure 10a) and b)). The more intense component at 4946.9 eV contains a relatively high percentage of Ti 3$p_{x/y/z}$ orbitals (7.6%) plus 60.8% C 2s AO based primarily on the Cp C atoms. The second Kβ'' peak at around 4952.0 eV contains some C 2s contribution but is composed mostly of Cl 3s AO mixed with Ti3p, in several contributions split over an energy range of 2 eV. The three highest intensity contributions to this Kβ'' peak are shown in Figure 10c)-e). As for Cp_2TiCl_2 a relatively broad K$\beta_{2,5}$ peak is due to a splitting in energy of the spectral components.

The theoretical structure of BisIn-$TiCl_2$ gives a good agreement between the experimental and theoretical spectra. Alongside this analysis, the experimental spectrum may also be understood via extrapolation from the

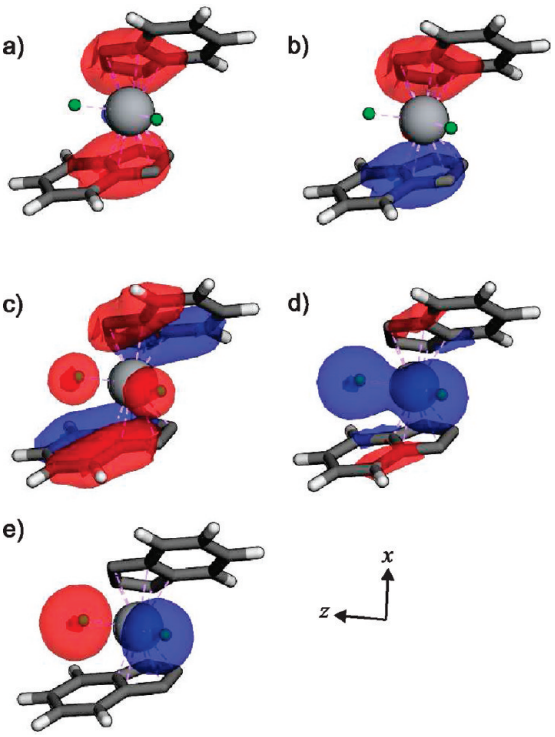

Figure 10. MOs of a theoretical BisIn-$TiCl_2$ molecule giving the main contributions to the Kβ'' peaks, from a) - c) C s orbitals and d), e) Cl s orbitals.

other compounds. The observed spectrum for BisIn-$TiCl_2$ is similar to that of Cp_2TiCl_2. This is reasonable to expect since the structures have several factors in common, *e. g* the Ti ligand atoms in both molecules are the same: two Cl atoms and two Cp rings. Also the measured Kβ'' peak attributed to C 2s -character MOs is slightly higher in intensity for BisIn-$TiCl_2$ than Cp_2TiCl_2, which is reasonable since there are two extra benzene rings per molecule in BisIn-$TiCl_2$ to increase the C 2s contribution (even though these atoms are not directly bonded to the Ti atom, there could be some Ti3p - $C_{benzene}$ 2s orbital overlap depending on the molecular geometry. Indeed from the calculated molecular structure of BisIn-$TiCl_2$ the peak at 4946.9 eV contains AO contributions from $C_{benzene}$2s, although this is a relatively weak proportion of the MO ($<8\%$ of the overall C2s AO contribution)).

THF-Containing Molecules. The two molecules Ti-$(THF)_2Cl_4$ and $Ti(THF)_3Cl_3$ contain oxygen in a different chemical environment to that of O in TiOPc, and this is evident in the valence-to-core XES spectra. No strong Kβ'' peak is seen in the range where a peak due to O would be expected. The DFT calculations place transitions relating to the O atoms at lower energy than for the TiOPc molecule, at 4944.8 eV for $Ti(THF)_2Cl_4$ and 4943.5 eV for $Ti(THF)_3Cl_3$. The broader/split K$\beta_{2,5}$ peak for $Ti(THF)_3Cl_3$ is reproduced in the calculations. Differences between the calculated and experimental spectra are mainly due to the broadening of low intensity Kβ'' peaks which appear smeared out in the experimental data.

The lack of a strong O based Kβ'' peak can be explained as relating to the degree of hybridization of the O 2s orbitals with the Ti 3p orbitals, and to some extent to the hybridization of the O orbitals over the THF rings.

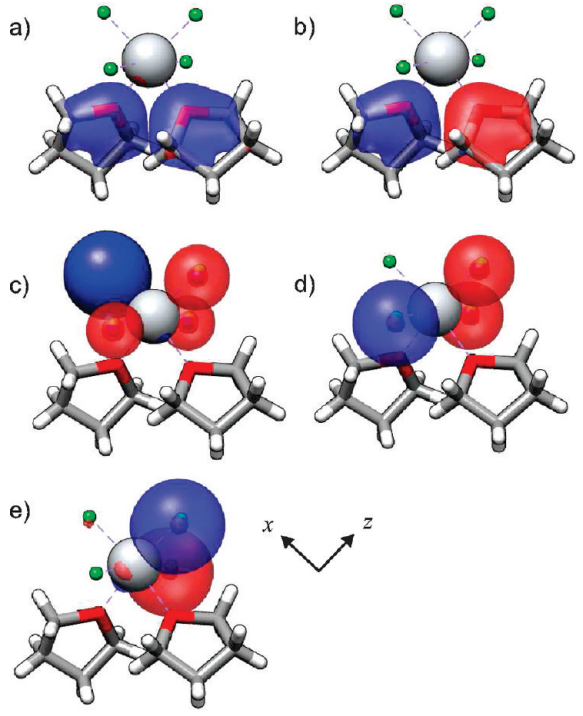

Figure 11. MOs of $Ti(THF)_2Cl_4$ giving the main contributions to the Kβ'' peaks, from a, b) O s orbitals and c)- e) Cl s orbitals.

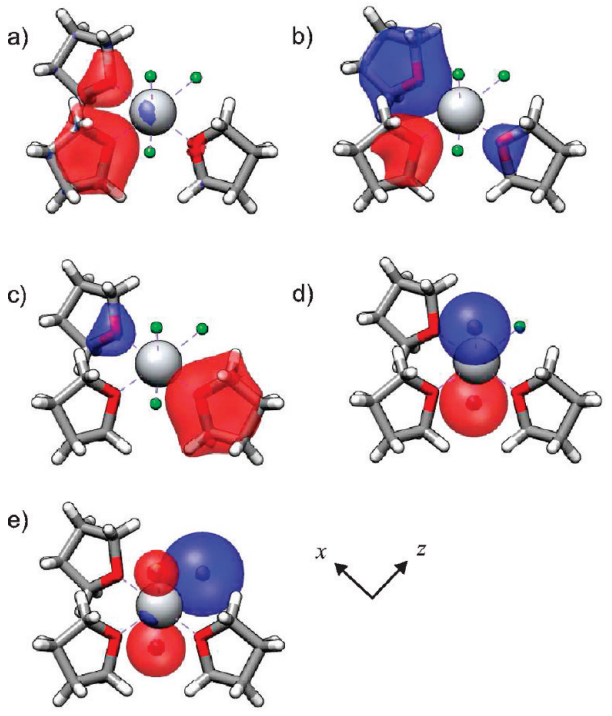

Figure 12. MOs of $Ti(THF)_3Cl_3$ giving the main contributions to the Kβ'' peaks, from a)- c) O s orbitals and d), e) Cl s orbitals.

The hybridization between O and Ti orbitals in the THF compounds is much weaker than that between Ti and O in TiOPc, for example. This is due in part to the Ti−O bond distance for the THF compounds, which is 2.0 ± 0.2 Å, much longer than that found in TiOPc. To study the hybridization effects the calculated MOs are useful. MOs a) and b) of $Ti(THF)_2Cl_4$ (Figure 11), which contribute to the O Kβ'' peak, have relatively pure O 2s character but relatively low Ti $3p_{x/y/z}$ character (lower than that seen for TiOPc for the main O 2s orbital). These MOs also have C 2s character from the two neighboring C atoms in the THF ring, which can be seen in the MO representation where the O based orbitals bridge over from the O to the two nearest C atoms in the THF ring as expected for a ring species. A similar orbital formation is seen for the $Ti(THF)_3Cl_3$ molecule which has three MOs relating to O 2s orbitals, a)- c), with strong O 2s character, some Ti 3p character, and also some C 2s character per MO from the two neighboring C atoms in each THF ring (Figure 12).

The Kβ'' peaks arising from Cl 3s -containing MOs in $Ti(THF)_2Cl_4$ are similar in energy position to those seen for the Cp-ring molecules, and are localized on the Cl atoms with some Ti 3p contribution. For $Ti(THF)_2Cl_4$, Cl s-based MOs shown in Figure 11c−e have Ti 4s and $3p_{x/y/z}$ character with a strong Cl 3s character over four Cl atoms. For $Ti(THF)_3Cl_3$ MOs (Figure 12d−e) are composed of Ti $p_{x/y/z}$ orbitals with strong contributions from Cl 3s orbitals over three Cl atoms. The measured Kβ'' peak due to Cl atoms is stronger in the $Ti(THF)_2Cl_4$ compound, which is reasonable as it has four Cl atoms compared to three and two in the other Cl-containing compounds studied.

The contribution from C atoms for these molecules does not give a strong Kβ'' signal for either molecule, which is not surprising as the C atoms are not directly bonded to the Ti atom. For $Ti(THF)_3Cl_3$, some C 2s orbitals hybridize with the Cl 3s based orbitals, and others (at lower energy) have very little hybridization with the Ti orbitals and thus do not give a large spectral intensity. For $Ti(THF)_2Cl_4$, all the C 2s orbitals lie at lower energy than the Cl 3s dominated MOs but have very little hybridization with Ti orbitals and therefore give very low intensity in the spectra.

Factors for Kβ'' Peak formation. Overall for the Ti molecules studied here, the factors found to affect the presence of Kβ'' peaks are bond length, the nature of the bonding interaction, the orbital hybridization over the molecule, and the symmetry arguments. These will be discussed in terms of the ligand types studied.

Kβ'' Peaks from O Atoms. The bond distance between the metal atom and the ligand has previously been found to play a key role in Kβ'' peak formation.[7,8] For TiOPc we see a clear Kβ'' peak from the O 2s orbital, where O is bonded to Ti through a relatively short bond of 1.64 Å. In $Ti(THF)_2Cl_4$ and $Ti(THF)_3Cl_3$, the Ti−O bond distance is larger than for TiOPc at 2.0 ± 0.2 Å, and a much weaker Kβ'' peak is seen. It can be seen from eq 1 that a shorter distance between the two participating atoms may act to increase the intensity of the Kβ'' peak observed, where a longer bond distance gives a lower intensity Kβ'' peak.

Another factor influencing the intensity of the Kβ'' peak seen due to O in these compounds is the hybridization of the MOs involved. In TiOPc, the O 2s orbital is strongly hybridized with the Ti $3p_z$ orbital (and Ti 4s and $3d_{z^2}$ orbitals) in a single MO without contribution from other atoms in the molecule. However, for $Ti(THF)_2Cl_4$ and $Ti(THF)_3Cl_3$, the Kβ'' peak is shown in the DFT calculations to arise from several MOs rather than a single MO, and these MOs do not only involve the Ti and O atoms. The O is present in a THF ring, and the calculated MOs show orbital

hybridization over the neighboring C atoms in the THF ring systems, giving a much weaker Kβ'' peak due to O.

Symmetry arguments also apply in the case of TiOPc, where spectral intensity can occur from the O atom which has 2s electrons mostly in a single MO with A_1 symmetry which can give spectral intensity, as the 1s core hole also has A_1 symmetry. This argument applies in the case of strict symmetry of the TiOPc molecule. Deviations between the calculated and experimental spectra arise, most likely due to a limitation in the size of the model used or the calculation method.

Kβ'' Peaks from N Atoms. The Ti−N bonding in (Pc) molecules is not via strong covalent interactions but is evenly distributed over the four N atoms through delocalized electrons to give a collective bonding interaction. The Ti−N bond length is also relatively large compared with those of other Ti−N systems. Weaker bonding interactions alongside longer bond distances means that no clear Kβ'' peaks are seen due to N atoms. It can also be seen from the calculations that there are no MOs which lie only over the Ti and N atoms; instead the MOs containing contributions from N s-type orbitals are spread over an energy range and are in highly hybridized MOs extending over the entire molecule. This delocalization means no strong ligand−metal orbital hybridization is present and no Kβ'' peaks are seen from N.

Kβ'' Peaks from C Atoms. In Cp-ring-containing molecules, some spectral intensity is observed in the Kβ'' region, shown in the calculations arising from Ti−C orbital hybridization, but the features are not well resolved. The Cp ring donates electron density to the Ti from the shared delocalized π electron orbital formed from the five member C atoms to form a bond. This collective electron donation from the ring carbons to the Ti gives a weaker Ti−C bond shared over five C atoms, which in turn gives a lower degree of hybridization between C s and Ti p orbitals, thus no sharp peak is observed. However, the calculations show that MOs involved in these C Kβ'' peaks only contain contributions from Ti and C, therefore it is not extensive hybridization over other types of atoms in the molecule (H or Cl) which causes the peak to be less well-defined, but it is the less direct nature of the C−Ti bond. Also, due to the low symmetry of the molecules, the Ti−C based MOs are split over an energy range which spreads the contributions over an energy range and gives a less well-defined peak from the C atoms.

Kβ'' Peaks from Cl Atoms. The spectrum of $TiPcCl_2$, compared with those of the other Cl-containing molecules, has a much less pronounced (almost non-observable) Kβ'' peak arising from MOs with Cl 3s character. In $TiPcCl_2$, there are only two MOs with strong Cl 3s and Ti 3p character, but not all Ti 3p (p_x, p_y, and p_z) orbitals are involved. In such low-symmetry molecules, it is necessary for the ligand ns orbital to hybridize with all three Ti 3p orbitals to maximize the overlap and give a stronger Kβ'' peak, particularly as the low symmetry acts to split up the MOs and cause peak broadening, making the peaks less clear. In all the Cl-containing molecules except $TiPcCl_2$, a Cl peak is seen, and the MOs contributing to the peak all contain both Cl 3s and Ti $3p_x$, $3p_y$, and $3p_z$ character orbitals.

Conclusions

The identification of ligands in Ti-containing molecules has been investigated using Kβ valence-to-core X-ray emission spectroscopy (XES). The presence of Kβ'' peaks depends upon several factors for these Ti molecules. We observe Kβ'' peaks dependent on the bond distance, the nature of the bonding interaction, the molecular symmetry, and the extent of delocalization of the relevant molecular orbitals (MOs) over the molecule. Density functional theory (DFT) calculations have been used to model the valence-to-core spectra and the high energy resolution fluorescence detection X-ray absorption near-edge spectroscopy (HERFD XANES) spectra of the compounds, thus showing the nature of the orbitals probed in these measurements.

The HERFD spectra show that strong p−d mixing is present in TiOPc due to the molecular symmetry. Weaker p−d mixing is observed for the other compounds, which have a split pre-edge peak. Probing the effect of the ligands via valence-to-core XES spectroscopy provides detailed information, alongside DFT calculations, to show how ligand s−Ti 3p orbital mixing takes place in different molecular systems.

A shorter bond distance is found to give a stronger Kβ'' peak, evident in comparing the strong O Kβ'' peak from TiOPc, which has a short Ti−O bond distance, with the much weaker O Kβ'' peaks of $Ti(THF)_2Cl_4$ and $Ti(THF)_3Cl_3$, with longer Ti−O bond distances. The peaks due to O are also weaker for the THF compounds as the O 2s-containing MOs involved are more delocalized and spread over the neighboring C atoms in the THF rings. Delocalization of the MOs also reduces the intensity of the Kβ'' peaks seen due to N in the (Pc) compounds where the relevant MOs are located over the entire molecule.

The nature of the ligand−Ti bond is also important to the presence of a Kβ'' peak. Stronger peaks are seen for O and Cl bonded directly to the Ti where ligand ns orbitals hybridize strongly with Ti 3p orbitals. Weaker, smeared out Kβ'' peaks are seen from C in Cp-ring-based molecules, in which the Cp ring bonds to the Ti via a π electron donation from the delocalized ring electrons. These considerations are vital when designing ligand identification experiments for molecular systems using Kβ valence-to-core XES.

Acknowledgment. The authors would like to thank T.-C. Weng (ESRF), E. Groppo (UNITO) and E. Gallo (UNITO) for assistance and useful discussions, C. Lapras (ESRF) for experimental support, and T. Petrenko and F. Neese (University of Bonn) for discussions and help with ORCA calculations.

Supporting Information Available: Calculations of Ti valence-to-core spectra for different TiOPc crystal structures; calculations of Ti valence-to-core spectra for different TiOPc cluster sizes; tables of calculated key MO spectral components for all molecules. This material is available free of charge via the Internet at http://pubs.acs.org.